JSR Publications

Available Online

J. Sci. Res. **17** (1), 259-271 (2025)

JOURNAL OF SCIENTIFIC RESEARCH

www.banglajol.info/index.php/JSR

Quantum Chemical Calculation and in-Silico A-Amylaze Inhibitory Prediction of *p*-Benzyloxy-based Prop-2-En-1-One

D. Santhiya, M. Durgadevi, G. Sundaraselvan*

Department of Chemistry, TK Govt. Arts College, Vridhachalam, Tamilnadu, India

Received 7 April 2024, accepted in final revised form 24 August 2024

Abstract

A chalcone namely (*E*)-3-(4-(benzyloxy)phenyl)-1-(4-methoxyphenyl)prop-2-en-1-one (4BPMP) has prepared from 4-benzyloxy benzaldehyde and 4-methoxyacetphenone by microwave method and the yield has obtained as higher. The IR and NMR spectra are recorded, and from these spectra, the functionality and α and β-protons/carbons are observed including the carbonyl group. The computational calculations for the title compound were carried out using the density functional theory (DFT) method with B3LYP (Becke's three-parameter exchange functional with the Lee-Yang-Parr) hybrid functional and 6-311++G(d,p) basis set. The structural parameters like bond lengths, bond angles, and dihedral angles were obtained from the optimized molecular geometry and discussed. The quantum chemical calculations showed that the 4BPMP molecule has a non-planar structure and possesses C1 point group symmetry. The frontier molecular orbital, molecular electrostatic surface potential, and global chemical reactivity parameters for the title molecule in the gas phase were reported and discussed. Based on the results, the synthesized molecule possesses good chemical strength and kinetic stability. The hyperpolarizability is greater than urea and pointed as a good NLO (Non-Linear Optical) material. Further, the α-amylase inhibitory behavior has been studied by docking method of the title compound with respective enzyme (pdb id : 1hny) and the results are well docked.

Keywords: Prop-2-en-1-one; DFT analysis; Molecular optimization; NLO prediction; In-silico α-amylase inhibitory study.

doi: https://dx.doi.org/10.3329/jsr.v17i1.72586 J. Sci. Res. **17** (1), 259-271 (2025)

1. Introduction

Chalcones or diarylpro-2-en-1-ones are important from the perspective of medicinal as well as synthetic chemistry. They are the building blocks for the synthesis of pharmacologically active agents [1] as well as the synthesis of novel organic molecules. Hence, they seek interest in the view of synthetic organic chemists. Chalcones are naturally occurring derivatives of the parent compound α,β- unsaturated ketone of the type 1,3-diarylprop-2-en-1-one belonging to the flavonoid family. Chemically they are open-chain flavonoids [2] in which two aromatic rings are held together by a three-carbon enone (-CO-CH=CH-) moiety.

* *Corresponding author*: drgsselvan@gmail.com

In addition, chalcones have interesting optical properties including non-linear optical responses [3] and these chalcones have potential applications in the areas of photonics, optoelectronics, optical information processing, frequency conversion, and telecommunication. The nonlinearity of the chalcone is due to the delocalization of the π-electron system connecting the donor-acceptor system across the molecule [4]. Claisen-Schmidt condensation [5] is known to be one of the most classical organic reactions through which chalcones can be synthesized. The presence of the alkene group in conjugation with carbonyl functionality is the principal reason behind the biological activities of chalcones [6]. Generally, they exhibited several biological properties like antimicrobial [7], anti-insect feedings [8], anti-malarial [9], antidiabetic [10], antiviral [11], anti-cancer [12], etc. They were prepared by the reaction of respective ketones with benzaldehydes via a crossed Aldol-condensation reaction. The titled compound has been synthesized to study its quantum chemical analysis and docking interactions and its IR and NMR spectra. The gas phase theoretical study has been ascertained for the compound using DFT calculations with B3LYP/6311++(d,p) basis set [13]. The structure has been optimized and its chemical reactivity and reactive sites are identified from HOMO-LUMO energies along with Mulliken charges. The NLO behavior of the titled molecule was also measured. The inhibition of α-glucosidase and α-amylase, enzymes involved in the digestion of carbohydrates, can significantly reduce the post-prandial increase of blood glucose and therefore can be an important strategy in the management of blood glucose levels in type-2 diabetic and borderline patients. The present article summarizes the developments in organic products like chalcones as α-amylase inhibitors. The inhibitory behavior of α-amylase enzyme by in-silico anti-diabetic activity [14] (pdb id : 1hny) has been performed using Auto dock vina and its best docking position has been identified.

2. Experimental

2.1. *Preparation of (E)-3-(4-(benzyloxy)phenyl)-1-(4-methoxyphenyl)prop-2-en-1-one (4BPMP)*

As per the various synthetic strategies available in the literature, the present compound has been prepared by microwave-assisted method for the purpose of its low time and excellent yield. Hence, the 4-benzyloxybenzaldehyde and 1-(4-methoxyphenyl)ethanone are taken as equal ratio and dissolved in 20 mL of absolute ethanol with a few drops of 10 % NaOH solution added [15] (Scheme 1). It was irradiated in a Microwave oven (640 W) for 2 mins and the completion of the reaction was checked by the TLC method. After completion of the reaction, the product was poured into ice water, filtered, and recrystallized in hot ethanol.

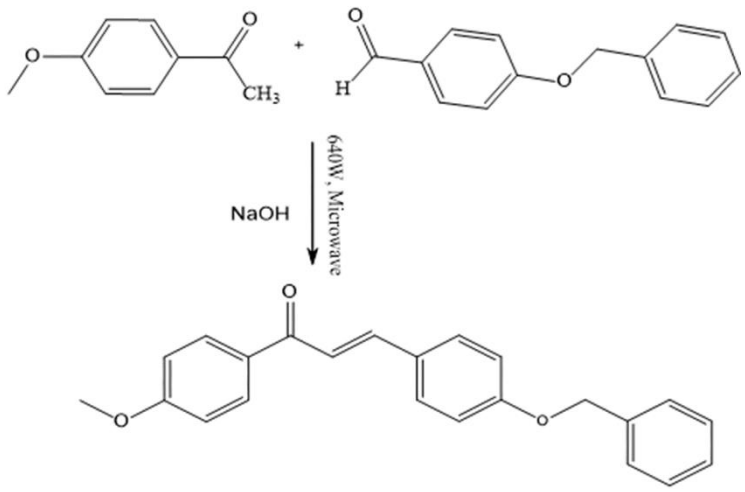

Scheme 1. Preparation of (E)-3-(4-(benzyloxy)phenyl)-1-(4-methoxyphenyl)prop-2-en-1-one (4BPMP).

2.2. *Spectral data of the titled compound*

Pale yellow solid; m.p. 124 °C; FT-IR (KBr; cm^{-1}): 2915.53, 2620.90, 1666.19 (carbonyl), 1596.77 (C=C), 1502.28, 1133.94 (CH_{ip}), 738.60 (CH_{op}), 1076.08 ($CH{=}CH_{op}$), 557.32 ($C{=}C_{op}$); δ^{1}Hppm (400 MHz; Choloroform-d): 8.026 (d, 2H), 7.772 (d, $1H_{\alpha}$, J = 15.6Hz), 7.586 (d. 2H), 7.444 – 7.391 (m, 5H), 7.353 (d, $1H_{\beta}$, J = 15.6Hz), 7.007 – 6.956 (m, 4H), 5.093 (s, 2H), 3.868 (3, 3H); δ^{13}Cppm (100 MHz; Choloroform-d): 188.71 (carbonyl), 163.27, 160.65, 143.72 (C_{α}), 136.44, 131.33, 130.69, 130.10, 128.15, 128.04, 119.66 (C_{β}), 115.25, 113.78, 70.78, 55.56.

2.3. *Computational details*

Density functional theory calculations were performed using the Gaussian-09 program package with no geometry constraints. The DFT/ B3LYP/6-311++G (d,p) method was used to optimize the geometry of the title molecules using the 6-311++G (d,p) basis set. The Gauss View 5.01 molecular visualization tool was used to create optimized geometry. The molecular electrostatic potential was computed using the same method to study the reactive sites of the title molecule. All of the computations were done in the gas phase for the optimized structure. The 6-311++G (d,p) basis set was used to calculate Mulliken atomic charges.

3. Results and Discussion

3.1. *Chemistry*

The present molecule **4BPMP** ((*E*)-3-(4-(benzyloxy)phenyl)-1-(4-methoxyphenyl)prop-2-en-1-one) molecule was synthesized via the Claisen–Schmit condensation reaction and the best yield (92 %) was gotten. The synthesized 4BPMP molecule was characterized by FT-IR, ^{13}C NMR, and ^{1}H-NMR spectroscopy (Fig. 1), and the findings were correlated with literature data. In the FT-IR spectra of synthesized chalcone, the appearance of peaks in the range of 2920-2887 cm^{-1} due to Ar-CH stretching vibrations [16].

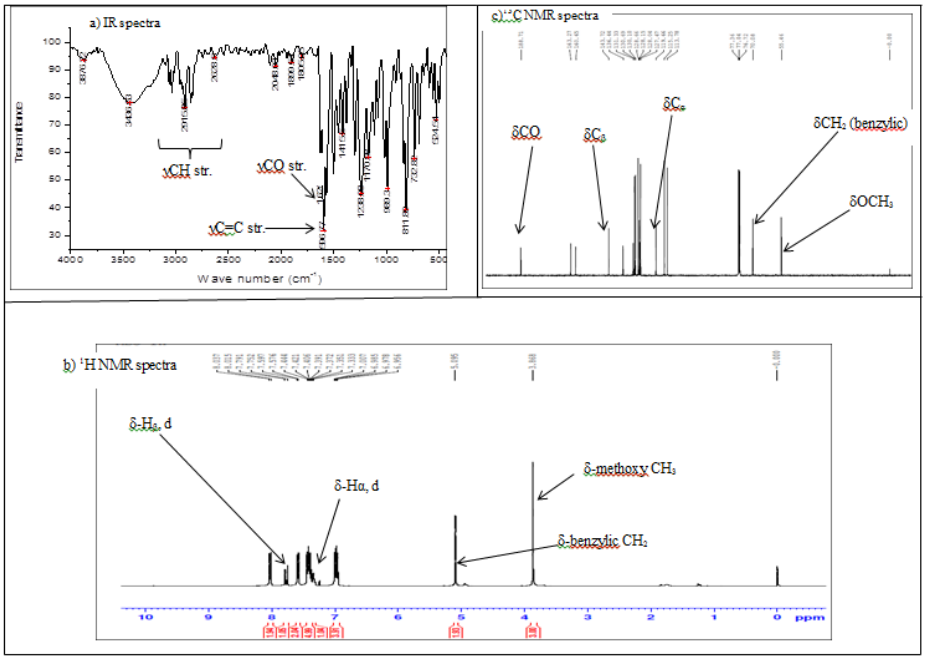

Fig. 1. Spectra for 4BPMP (**a**: IR; **b**: ^{1}H NMR and **c**: ^{13}C NMR).

The intense peak at 1666.19 cm^{-1} is due to *ν*CO stretching. The carbonyl peak was observed at a lower wavenumber than a normal ketone carbonyl peak in the infrared spectra due to the existence of a ketonic carbonyl group conjugated with the olefinic carbon-carbon double bond. The olefinic group (-C=C-) is observed at 1596.77 cm^{-1}. The ^{1}H NMR coupling constant analyses indicated that hydrogen atoms of the olefinic carbon-carbon bond were in a *trans* configuration (J approximately 15Hz). The methylene (CH_2) group of the benzyloxy part of the synthesized chalcone appeared at 5.093 ppm and the methoxy proton appeared at 3.868 ppm. The signals for these methylene (CH_2) and methyl (OCH_3) groups can also be observed in the ^{13}C NMR spectrum at 72.05 and 29.23 ppm. Additionally, multiplets in the aromatic region (6.80-8.00 ppm) indicate the presence of aromatic protons in the compound. The ^{13}C NMR signal at approximately 188.71 ppm in the synthesized compound concerns to α,β-unsaturated carbonyl carbon. Despite the fact that the ketone absorbs approximately 200 ppm, the existence of unsaturation leads to a slight uprooting to the high field, and the reasonable cause is charge delocalization by the

benzene ring or by the double bond, which makes the carbonyl carbon less electron deficient.

3.2. *Computational study*

3.2.1. *Molecular structure study*

The 4BPMP molecule was analyzed in the current examination using the density functional theory method with a B3LYP/6-311++G(d,p) basis set to build up different structural and chemical parameters. 4BPMP is a non-planer molecule with C1 point group symmetry, as predicted by the DFT analysis. Fig. 2 depicts the optimized molecular structure.

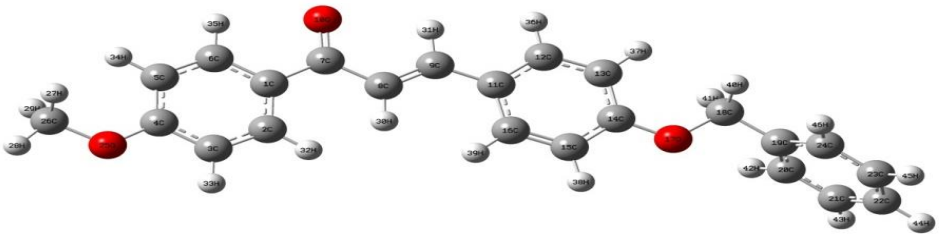

Fig. 2. Optimized structure of 4BPMP by DFT method.

The bond length and bond angle data of **4BPMP** are given in Table 1. In the 4BPMP compound, all the phenyl C-C bond lengths are observed at ~1.4A°, the carbonyl bond (C7-O10) length is 1.261 Å and the olefinic bond length (C8-C9) is 1.351 Å. This bond length favored the existence of a double bond character. All other bond length values show good agreement with the structure of the titled molecule. The bond angle between C7-C8-C9 bonds is 120.653°. From Table 1, the methyl group lay in the same plane and the benzyloxy group lay in non–planar with Chalcone. Similarly, other bond angle data are rightly matching with the various bond angles of the titled molecule. The dihedral angle for 7C-8C-9C-11C is calculated as -179.772° which indicates the *E*-conformation of the molecule.

3.2.2. *Non-Linear Optical (NLO) properties*

In different fields, non-linear optical materials have different applications [17], evolving outstanding properties such as frequent shift, optical modulation, optical switching, etc. The total dipole moment (μ_{tot}) of 4BPMP was calculated at 2.1208 D. The higher dipole moment will indicate a higher electron density which will lead to a greater charge transfer [18]. The higher the dipole moment, the higher the first polarizability will indicate the higher NLO properties [19]. Moreover, the calculated values of hyperpolarizability (β_0) and linear polarizability (α_{tot}) of the compound were 2.152×10^{-30} esu and 20.040×10^{-24} esu respectively. The polarisabilty value of the titled compounds is higher than the standard

urea (Table 3). Therefore, we can conclude that the synthesized compound has excellent candidate NLO materials.

Table 1. Selected bond lengths, bond angles, and dihedral angles of 4BPMP calculated by DFT method.

Bond length (A°)		Bond angle (°)		Dihedral angle (°)	
1C-2C	1.410	1C-2C-3C	121.016	1C-2C-3C-4C	0.032
2C-3C	1.389	2C-3C-4C	119.974	2C-3C-4C-5C	-0.074
3C-4C	1.401	3C-4C-5C	120.069	3C-4C-5C-6C	0.022
4C-5C	1.401	4C-5C-6C	119.348	5C-6C-1C-7C	-179.974
5C-6C	1.392	6C-1C-7C	117.825	6C-1C-7C-8C	-178.248
1C-7C	1.490	1C-7C-8C	120.064	1C-7C-8C-9C	-179.678
7C-8C	1.473	7C-8C-9C	120.653	6C-1C-7C-10O	1.575
8C-9C	1.351	1C-7C-10O	119.393	7C-8C-9C-11C	-179.772
7C-10O	1.261	8C-9C-11C	128.193	8C-9C-11C-12C	179.818
9C-11C	1.458	9C-11C-12C	118.939	9C-11C-12C-13C	-179.910
11C-12C	1.407	11C-12C-13C	121.930	11C-12C-13C-14C	-0.017
12C-13C	1.396	12C-13C-14C	119.276	12C-13C-14C-15C	-0.014
13C-14C	1.399	13C-14C-15C	119.943	13C-14C-15C-16C	0.023
14C-15C	1.405	14C-15C-16C	120.152	12C-13C-14C-17O	-179.953
15C-16C	1.384	13C-14C-17O	124.774	13C-14C-17O-18C	-0.870
14C-17O	1.389	14C-17O-18C	119.210	14C-17O-18C-19C	-179.468
17O-18C	1.473	17O-18C-19C	107.617	17O-18C-19C-20C	83.452
18C-19C	1.502	18C-19C-20C	120.394	18C-19C-20C-21C	-178.798
19C-20C	1.402	19C-20C-21C	120.546	19C-20C-21C-22C	0.046
20C-21C	1.396	20C-21C-22C	120.016	20C-21C-22C-23C	0.154
21C-22C	1.398	21C-22C-23C	119.844	21C-22C-23C-24C	-0.060
22C-23C	1.397	22C-23C-24C	119.992	2C-3C-4C-25O	179.938
23C-24C	1.397	3C-4C-25O	115.501	3C-4C-25O-26C	179.920
4C-25O	1.387	4C-25O-26C	119.348		
25O-26C	1.454				

Table 2. Dipole moment (μ), polarizability (α_0) and hyperpolarizability (β_0) of 4BPMP by DFT method.

Dipole vector components	Dipole moment, μ (Debye)	Parameters	Hyperpolarizability
μ_x	-1.6634	β_{xxx}	321.278
μ_y	-1.3146	β_{xxy}	-46.883
μ_z	0.0519	β_{xyy}	-43.261
μ_{total}	2.1208	β_{yyy}	-12.120
Parameters	**Polarizability**	β_{xxz}	-0.242
α_{xx}	-94.913	β_{xyz}	6.126
α_{xy}	-8.969	β_{yyz}	0.870
α_{yy}	-157.063	β_{xzz}	-37.024
α_{xz}	0.729	β_{yzz}	-4.232
α_{yz}	-0.764	β_{zzz}	0.387
α_{zz}	-153.694	$\beta_{\tau o \tau}$ (α.υ)	249.153
<α> (a.u)	135.223	β_o(esu) x 10^{-30}	2.152
α_{tot} (esu) x 10^{-24}	20.040		

3.2.3. *Frontier molecular orbital*

The optoelectronic parameters of the structure of the title compound were obtained using Frontier theory at the B3LYP/6-31++G (d,p) basis set. Frontier Molecular Orbital (FMOs) such as highest occupied molecular orbital (HOMO) and lowest unoccupied molecular orbital (LUMO) has been used to draw useful information on the optoelectronic properties of various organic molecules [20]. The electron donors will be present in HOMO and the innermost orbital unoccupied by the electrons performs as the electron acceptor. E_{HOMO} has the electron-donating capability of the molecule. The greater the HOMO energy, the more will be the electron-donating capability. The energy gap ΔE= 3.984eV between the HOMO, and LUMO orbital (Table 3) indicates the reactivity and stable structure of the molecule. As shown in Fig. 3, HOMO predominantly occupies the central α,β-unsaturated ketone, and aldehydic phenyl moieties except the benzyloxy moiety. LUMO occupies the same trend as HOMO with the inclusion of *p*-methoxyphenyl moiety of the ketone. In addition, the energy gap between HOMO-1 and LUMO+1 is 5.638eV. Moreover, the lower the HOMO and LUMO energy gap explains the eventual charge transfer interactions taking place within the molecule.

Density functional theory-based global chemical reactivity descriptors like Chemical hardness, chemical softness, electronegativity, chemical potential, electrophilicity index, etc. are calculated from HOMO and LUMO energies [21] and are given in Table 4. Global chemical reactivity descriptors are used to understand the relationship between structure, stability, and global chemical reactivity of compounds.

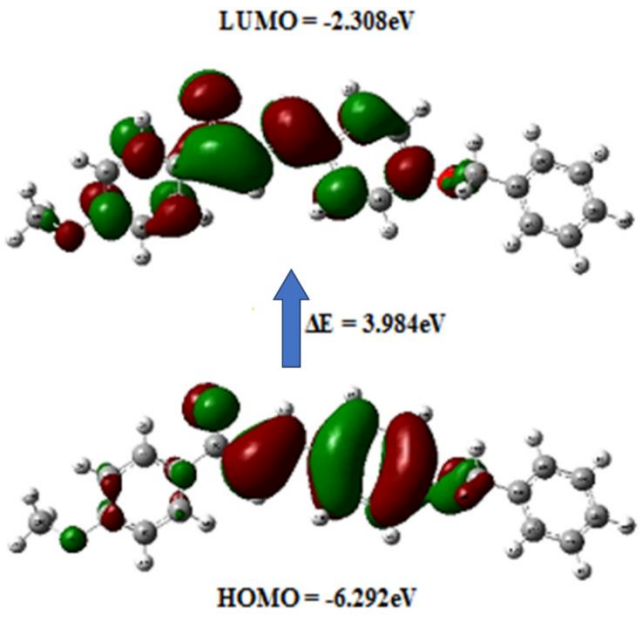

Fig. 3. HOMO – LUMO energy diagram of 4BPMP by DFT method.

In accordance with the HSAB principle, normally the molecule with the least value of global hardness is expected to have the highest inhibition efficiency [22]. In our present study, it is clear from the calculation that the 4BPMP compound having the lowest hardness value and highest softness value suggests that more reactive and expected to be the best inhibitor [23].

Table 3. Electronic and Global descriptors of 4BPMP by DFT method.

Electronic Parameters	4BPMP
E_{HOMO} (eV)	-6.292
E_{LUMO} (eV)	-2.308
Energy gap (eV)	3.984
Ionization energy (I)	6.292
Electron affinity (A)	2.308
Global reactivity parameters	
Global hardness (η)	1.992
Chemical potential (μ)	-4.300
Electrophilicity index (ω)	4.641
Electronegativity (χ)	4.322
Chemical softness (s)	0.502

Table 3 revealed that the present molecule has a higher global electrophilicity index (4.641 eV), signifying that it is more likely to accept electrons and nucleophilic attack. The calculated chemical potential (-4.3006 eV) and the electrophilicity index indicate that the 4BPMP molecule possesses excellent chemical strength and stability. Additionally, the title compound has a high electrophilicity index which highlights the biological activity of the compound [24].

3.2.4. *Mulliken atomic charges and molecular electrostatic potential studies*

In view of the atomic charge effect, dipole moment, molecular polarizability, electronic structure, and many properties of molecular structures, Mulliken atomic charge calculation has a key role in the application of quantum chemical approximation to molecular frameworks [25]. The distributions of charge over the atoms represent the existence of pairs of donors and acceptors enabling the transfer of charge in the molecules. The Mulliken population analysis as displayed in Table 4, for the 4BPMP molecule was derived using the 6-311++G(d,p) basis of the B3LYP stage. The charge distribution in the 4BPMP molecule indicates that all hydrogen atoms are positively charged while the magnitudes of the carbon atomic charges are found to be both positive and negative. C26 is the carbon with the largest positive charge (0.284). The attachment to oxygen is the cause behind its high atomic charge content. The charges on all the three oxygen atoms (O10, O17, O25) are negative. The respective column chart is given in Fig. 4.

Table 4. Mulliken population charges of 4BPMP by DFT method.

Atoms	Charges	Atoms	Charges
1C	-0.132	14C	-0.020
2C	0.117	15C	0.090
3C	-0.039	16C	0.128
4C	0.272	17O	-0.508
5C	0.006	18C	0.018
6C	0.081	19C	0.067
7C	0.174	20C	-0.008
8C	0.033	21C	0.028
9C	0.007	22C	-0.009
10O	-0.399	23C	0.053
11C	0.001	24C	0.268
12C	0.009	25O	-0.518
13C	0.002	26C	0.284

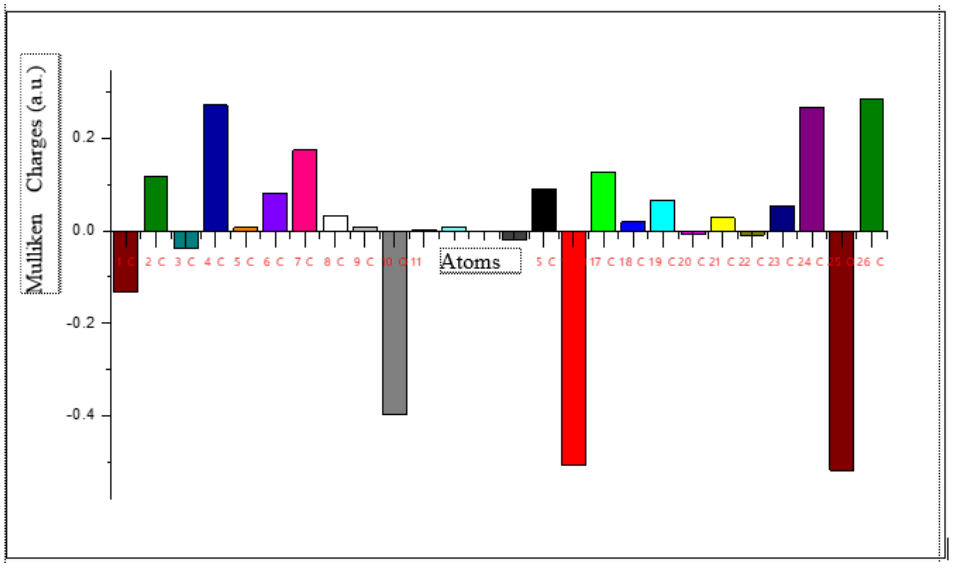

Fig. 4. Column chart of Mulliken charges of 4BPMP by DFT method.

At the B3LYP/6-311++G(d,p) level of theory, the MESP (Molecular Electrostatic Potential) surface and electrostatic potential values were calculated. Fig. 5 shows the MESP plotted for each of the three chalcones. MESP's importance stems from the fact that it simultaneously reveals molecular size, and shape, as well as positive, negative, and neutral electrostatic potential regions in terms of color differentiation, and it's critical for studying the interaction between molecular structure and its physio-chemical properties [26]. The different colors represent different features of the electrostatic potential on the surface; red represents places with the largest electro-negative electrostatic potential, blue represents the most positive electrostatic potential, and green represents zero potential. The potential increases in the following order: red, orange, yellow, green, blue. The most electropositive region (blue region, electron-poor) is placed over the hydrogen atoms of phenyl rings,

whereas the most electronegative region (red region, electron-rich) is located over the oxygen atoms [27], according to the MESP plots.

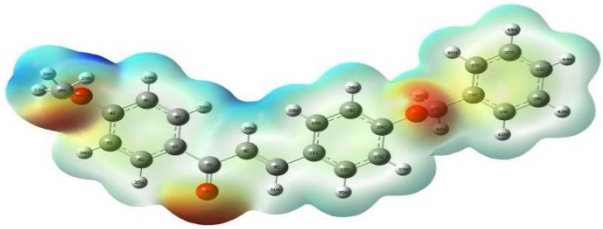

Fig. 5. Molecular Electrostatic Potential Distribution of 4BPMP by DFT method.

3.3. *Molecular docking procedure*

Molecular docking studies is a search algorithm for the best orientation of the small molecules known as ligand which perfectly fits into the target protein's cavity and therefore plays a vital role in drug design and therapy. It is also used to analyze the affinity and binding orientation of the molecule with the target. In this present study, a graphical tool known as Auto Dock suite 1.5.6 (ADT) is used to predict how the ligand binds with a receptor in 3D.

3.3.1. *Protein setup*

The crystal structure of (PDB ID: 1HNY) [28], was obtained from the RCSB Protein Data Bank [29]. All the water, non-interacting ions, and cocrystallized inhibitors were removed. AutoDockTools (Version 1.5.6) was used to prepare the proteins for molecular docking. Polar hydrogens were added, Gasteiger charges and Kollman charges were calculated to examine its minimum binding energy, and the generated PDBQT files were saved. Centers were constructed using grid box parameters in AutoDockTools.

3.3.2. *Ligand setup*

The 3D structure of **4BPMP** was prepared by ChemDraw Pro12.0 software. [Chemical Structure Drawing Standard: Cambridge Soft Corporation, USA (2010)]. Auto Dock tools were used to dock, the ligand into the active sites. The title compound acting as a ligand was computed with partial charges by the Geistenger method. The ligand was added with torsion information depending on which torsions need to be rotated during docking and was saved in PDBQT format.

3.3.3. *Docking against α-amylaze enzyme*

The docking parameters namely binding energy (kcal/mol), inhibition constant (lm), and intermolecular energy (kcal/mol) of the 4BPMP molecule with respect to the target protein

is tabulated in Table 5. The best-docked conformation was analyzed by the minimum binding energy of the **4BPMP** molecule with the residue of the proteins of α-amylase (1HNY) is presented in Fig. 6. The chalcone fits tightly into the inhibition site of the 1HNY protein [30] forming three hydrogen bonds (H-bonds) with residues ASN137, LEU162 and ASP206. The oxygen atom in the methoxy group has a strong fitting tendency with ASN137 protein residue with the shortest distance of 2.578 Å. Similarly, the oxygen atom of the carbonyl group in α,β-unsaturated ketone docked with LEU162 residue in a good manner. The carbon atom of the methyl group also formed a hydrogen bond with ASP206 residue. The oxygen atoms in carbonyl and methoxy groups behave as H-bond acceptors for the active-site residues. In addition, other interactions like hydrophobic interactions are also observed between the titled molecule and the selected protein residue. The π-electrons of the phenyl groups of present molecules are shown two hydrophobic interactions. The alkyl groups of ALA198 and, LYS200 have also shown interactions by their alkyl groups with the phenyl rings of the present molecule under study.

Table 5. Molecular Docking Results of 4BPMP.

Binding affinity (Kcal/mL)	Type of interaction	Distance (Å)	Interacting Residues
-9.2	Hydrogen Bond	2.578	ASN137
	Hydrogen Bond	2.698	LEU162
	Hydrogen Bond	3.563	ASP206
	Hydrophobic	3.648	LEU162
	Hydrophobic	3.652	ILE235
	Hydrophobic	4.469	ALA198
	Hydrophobic	4.456	LYS200
	Hydrophobic	4.526	ALA198

The least value of the inhibition constant gives the minimum value for binding energy which indicates the increase in biological activity and hence lower dosage of the drug for clinical trials. These results highlight that a stable complex is formed from the docked ligand with the target proteins and hence makes the title compound a suitable drug for various α-amylase inhibitory diabetic treatments. Further experimental analysis is required to validate this point.

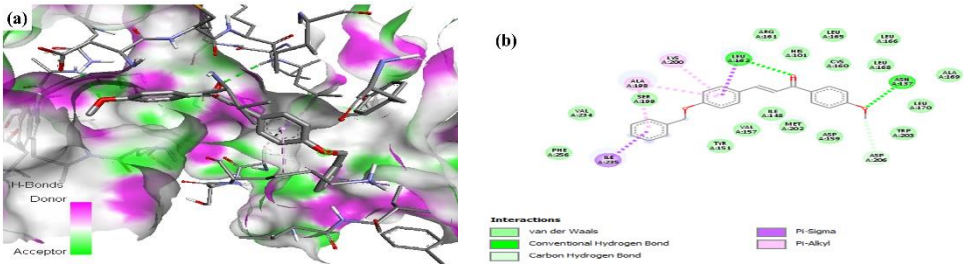

Fig. 6. Molecular docking images of 1HNY with 4BPMP (a:3D view; b:2D view).

4. Conclusion

In the present study, a *para*-substituted benzyloxy-based Chalcone (4BPMP) has been prepared by adopting the Microwave method. It has been characterized by their IR and NMR spectra. A comparative study of experimental and theoretical investigations on the optimized structure was found to be in good agreement with the title molecule. The significant variation in HOMO -LUMO energies supports polarization within the molecule and further the high electrophilicity index and least value of softness confirm the 4BPMP is biologically active. MEP and Mulliken's calculations revealed the positive and negative sites within the molecule. Due to its higher polarizability and hyperpolarizability than urea, it is stated as a good NLO material. Further, molecular docking for the title molecule on α-amylase enzyme was done using Auto Dock suite software. These results showed that title Chalcone can be used as an effective antidiabetic drug because of its good binding affinity which may be effective in inhibition of alpha amylase enzyme. Hence the title compound paves the way for clinical chemists to proceed further research in chalcone drug design.

Acknowledgment

The authors wished to thank the IR and NMR Facility, IACC, Gandhigram Rural Institute, Gandhigram, for recording the NMR and IR spectra of all compounds. Also thanks to PG & Res. Dept. of Chemistry, TK Govt. Arts College, Vridhachalam for providing facilities.

Reference

1. C. Zhuang, W. Zhang, C. Sheng, W. Zhang, C. Xing, and Z. Miao, Chem. Rev. **117**, 7762 (2017). https://doi.org/10.1021/acs.chemrev.7b00020
2. T. Barberán, A. Francisco, Clifford, and N. Michael, J. Sci. Food. Agri. **80**, 1073 (2000). https://doi.org/10.1002/(SICI)1097-0010(20000515)80:7<1073::AID-JSFA568>3.0.CO;2-B
3. H. Pir, N. Gunay, Ö. Tamer, D. Avc, and Y. Atalay, Spectrochim. Acta **112A**, 331 (2013). https://doi.org/10.1016/j.saa.2013.04.063
4. A. Barakat, A. M. Al-Majid, S. M Soliman, Y. N. Mabkhot, M Ali et al., Chem. Central J. **9**, ID 35 (2015). https://doi.org/10.1186/s13065-015-0112-5
5. L. Claisen and A. Claparede, Ber. Dtsch. Chem. Ges. **14**, 2460 (1881). https://doi.org/10.1002/cber.188101402192
6. P. Singh, A. Anand, and V. Kumar, Eur. J. Med. Chem. **85**, 78 (2014). https://doi.org/10.1016/j.ejmech.2014.08.033
7. N. V. Sadgir, S. L. Dhonnar, B. S. Jagdale, and B. A. B. Sawant, SN App. Sci. **2**, 1376 (2020). https://doi.org/10.1007/s42452-020-2923-9.
8. A. E. Aiwonegbe and J. U. Iyasele, J. Chem. Soc. Nigeria **47**, 18 (2022).
9. H. -L.Qin, Z-W. Zhang, R. Lekkala, H. Alsulami, and K. Rakesh, Eur. J. Med. Chem. **193**, ID 112215 (2020). https://doi.org/10.1016/j.ejmech.2020.112215
10. P. Shukla, M. Satyanarayana, P. C. Verma, J. Tiwari, A. P. Dwivedi et al., Curric. Sci. **12**, 1675 (2017). https://doi.org/10.18520/cs/v112/i08/1675-1689
11. Z. Wan, D. Hu, P. Li, D. Xie, and X. Gan, Molecules **20**, 1186 (2015). https://doi.org/10.3390/molecules200711861
12. Y. Ouyang, J. Li, X. Chen, X. Fu, S. Sun, and Q. Wu, Biomolecules **11**, 894 (2021). https://doi.org/10.3390/biom11060894
13. D. Shyamala, R. Rathikha, and K. Gomathi, Int. J. Pure and Appl. Phys. **12**, 3 (2016).

14. M. Ali, M. Khan, K. Zaman, A. Wadood, M. Iqbal et al., Med. Chem. **17**, 903 (2021). https://doi.org/10.2174/1573406416666200611103039
15. S. Yadav, A. Khare, K. K. Yadav, P. C. Maurya1, A. K. Singh, and A. Kumar, J. Sci. Res. **14**, 79 (2022). https://doi.org/10.3329/jsr.v14i1.53339
16. P. S. Raghu, World J. Pharm. Res. **6**, 1244 (2017).
17. M. N. Arshad, A. M. Al-Dies, A. M. Asiri, M. Khalid, A. S. Birinji et al., J. Mol. Struc. **1141**, 124 (2017). https://doi.org/10.1016/j.molstruc.2017.03.090
18. M. Khalid, A. Ali, R. Jawaria, M. A. Asghar, S. Asim et al., RSC Adv. **10**, 22273 (2020). https://doi.org/10.1039/D0RA02857F
19. A. H. Anizaim, S. Arshad, M. F. Zaini, M. Abdullah, D. A. Zainuri, and I. A. Razak, Opt. Mat. **98**, ID 109406 (2019). https://doi.org/10.1016/j.optmat.2019.109406
20. J. C. Phillips, Phys. Rev. **123**, 420 (1961). https://doi.org/10.1103/PhysRev.123.420
21. N. R. Sheela, S. Muthu, and S. Sampathkrishnan, Spectrochim. Acta Part A: Mol. Biomol. Spectro. **120**, 237 (2014). https://doi:10.1016/j.saa.2013.10.007
22. E. E. Ebenso, D. A. Isabirye, and N. O. Eddy, Int. J. Mol. Sci. **11**, 2473 (2010). https://doi.org/10.3390/ijms11062473
23. P. Udhayakala, J. Chem. Pharm. Res. **7**, 803 (2015).
24. R. Parthasarathi, J. Padmanaban, M. Elango, V. Subramanian, and P. K. Chattaraj, Chem. Phys. Lett. **394**, 225 (2004). https://doi.org/10.1016/j.cplett.2004.07.002
25. D. A. Zainuri, I. A. Razak, and S. Arshad, Acta Cryst. E **74**, 780 (2008). https://doi:10.1107/S2056989018006527
26. S. Sebastien and N. Sundaraganesan, Spectrochim. Acta **75**(A), 941 (2010). https://doi.org/10.1016/j.saa.2009.11.030
27. R. Subha and N. Ingarsal, J. Sci. Res. **15**, 887 (2023). https://doi.org/10.3329/jsr.v15i3.64498
28. A. Thamarai, R. Vadamalar, M. Raja, S. Muthu, B. Narayana et al., J. Mol. Struct. **1202**, 127349 (2020). https://doi.org/10.1016/j.molstruc.2019.127349
29. G. D. Brayer, Y. Luo and S. G. Withers, Protein Sci. **4**, 1730 (1995). https://doi.org/10.1002/pro.5560040908
30. R. Nithyabalaji, R. M. P. Ramya, R. Kavitha, K. Radhakrishnan, J. V. Kumar et al., Chem. Phys. Impac. **8**, ID 100422 (2024). https://doi.org/10.1016/j.chphi.2023.100422